

# We are IntechOpen, the world's leading publisher of Open Access books Built by scientists, for scientists

6,900

Open access books available

185,000

International authors and editors

200M

Downloads

Our authors are among the

154

Countries delivered to

TOP 1%

most cited scientists

12.2%

Contributors from top 500 universities



WEB OF SCIENCE™

Selection of our books indexed in the Book Citation Index  
in Web of Science™ Core Collection (BKCI)

Interested in publishing with us?  
Contact [book.department@intechopen.com](mailto:book.department@intechopen.com)

Numbers displayed above are based on latest data collected.  
For more information visit [www.intechopen.com](http://www.intechopen.com)



---

# Ordovician and Carboniferous Volcanism/Plutonism in Central Inner Mongolia, China and Paleozoic Evolution of the Central Asian Orogenic Belt

---

Yuruo Shi

Additional information is available at the end of the chapter

<http://dx.doi.org/10.5772/62303>

---

## Abstract

Adakite was originally proposed as a genetic term to define intermediate to high silica, high Sr/Y and La/Yb volcanic and plutonic rocks derived from melting of young, subducted lithosphere. However, most volcanic rocks in modern island arcs and continental arcs are probably derived from melting in the mantle wedge. Trace element chemistry with high Sr/Y ratios is a distinguishing characteristic of adakites. Ordovician and Carboniferous volcanic/plutonic rocks with high Sr/Y ratios occur in Central Inner Mongolia, which is situated on the southern margin of the Central Asian Orogenic Belt (CAOB). The samples are mostly granodiorite, tonalite and quartz-diorite in composition with intermediate to high-silica, high Na<sub>2</sub>O (3.08–4.26 wt.%), low K<sub>2</sub>O (0.89–2.86 wt.%) and high Na<sub>2</sub>O/K<sub>2</sub>O and Sr/Y ratios. Their chondrite-normalized REE patterns are characterized by LREE enrichment. In mantle-normalized multi-element variation diagrams, they show typical negative Nb anomalies, and all samples display positive  $\epsilon_{\text{Hf}}(t)$  and  $\epsilon_{\text{Nd}}(t)$  values, and low  $I_{\text{Sr}}$ . The Ordovician rocks, however, show higher Sr/Y and La/Yb ratios than the Carboniferous samples, implying that the older granitoids represent adakitic granitoids, and the Carboniferous granitoids are typical subduction-related arc granitoids but also with adakite-like compositions. The results are compatible with the view that the Central Asian Orogenic Belt (CAOB) in Inner Mongolia evolved through operation of several subduction systems with different polarities: an early-middle Paleozoic subduction and accretion system along the northern margin of the North China Craton and the southern margin of the Mongolian terrane, and late Paleozoic northward subduction along the northern orogen and exhumation of a high-pressure metamorphic terrane on the northern margin of the North China Craton.

**Keywords:** Adakitic, Ordovician and Carboniferous, Geochemistry, Hf-in-zircon isotopes, Central Inner Mongolia, CAOB

## 1. Introduction

It is generally agreed that the Solonker suture zone represents the southernmost termination of the Central Asian Orogenic belt (CAOB; [1–5]). However, there are a lot of controversies about the timing of the amalgamation of the Central Asian Orogenic belt with continental blocks to the south [1–9]. It is still debated whether the CAOB evolved through subduction and accretion of a single, long-lasting, subduction system [10] or through several subduction systems with different polarities and through collision/accretion of arcs and microcontinents [11–15].

Adakite was originally proposed as a genetic term to define intermediate to high-silica, high Sr/Y and La/Yb volcanic and plutonic rocks derived from melting of young, subducted lithosphere [16]. However, most volcanic rocks in modern island arcs and continental arcs are probably derived from melting in the mantle wedge [17]. Trace element chemistry with high Sr/Y ratios is a distinguishing characteristic of adakites [16, 18]. Ordovician and Carboniferous volcanic/plutonic rocks with high Sr/Y ratios occur in Central Inner Mongolia, which is situated on the southern margin of the Central Asian Orogenic Belt (CAOB, [19]). Early Paleozoic [6–9, 20–22] and Late Paleozoic [2–4, 23] arc volcanism/plutonism as part of trench-island arc-basin systems occurred along the southern margin of South Mongolian microcontinent and the northern margin of North China Craton, suggesting concurrent two-way subduction towards opposing continental margins. The chapter focuses on early and late Paleozoic volcanic/plutonic rocks with high Sr/Y ratios in Central Inner Mongolia, and contributes geochemical data to the evolution of the CAOB.

## 2. Geotectonic situation

Central Asian Orogenic Belt (CAOB, [19]) is a giant accretionary orogen [15], bounded by the Siberian, Tarim and North China Craton ([19, 24]; **Figure 1**), and reflects a complex evolution from the late Mesoproterozoic to late Palaeozoic [1, 6, 8, 14, 26, 27].

In Central Inner Mongolia and adjacent southern Mongolia, the Solonker suture zone can be traced for ca. 1000 km by dismembered ophiolite fragments (**Figure 1**) and represents a major paleo-plate boundary in Central Asia that stretches northeastwards for more than 2500 km in Mongolia and China [28]. It has been variably interpreted as the southernmost limit of the Altaiids ([10]) or the southernmost termination of the CAOB [1]. The Solonker suture zone separates two continental blocks (**Figure 1**) [3]. The Northern Block consists of the Southern Mongolia (or Hutag Uul) block (gneissic granite,  $1784 \pm 7$  Ma, Shi et al., unpublished data) and the Northern Orogen, which includes metamorphic complex (an orthogneiss has a zircon age of  $437 \pm 3$  Ma, [29]), an ophiolitic mélangé with blueschist, a near-trench granitoid (ca. 498–461 Ma) and a juvenile arc (ca. 484–469 Ma, [3]). The Southern Block comprises the southern orogen and the northern margin of the North China Craton.

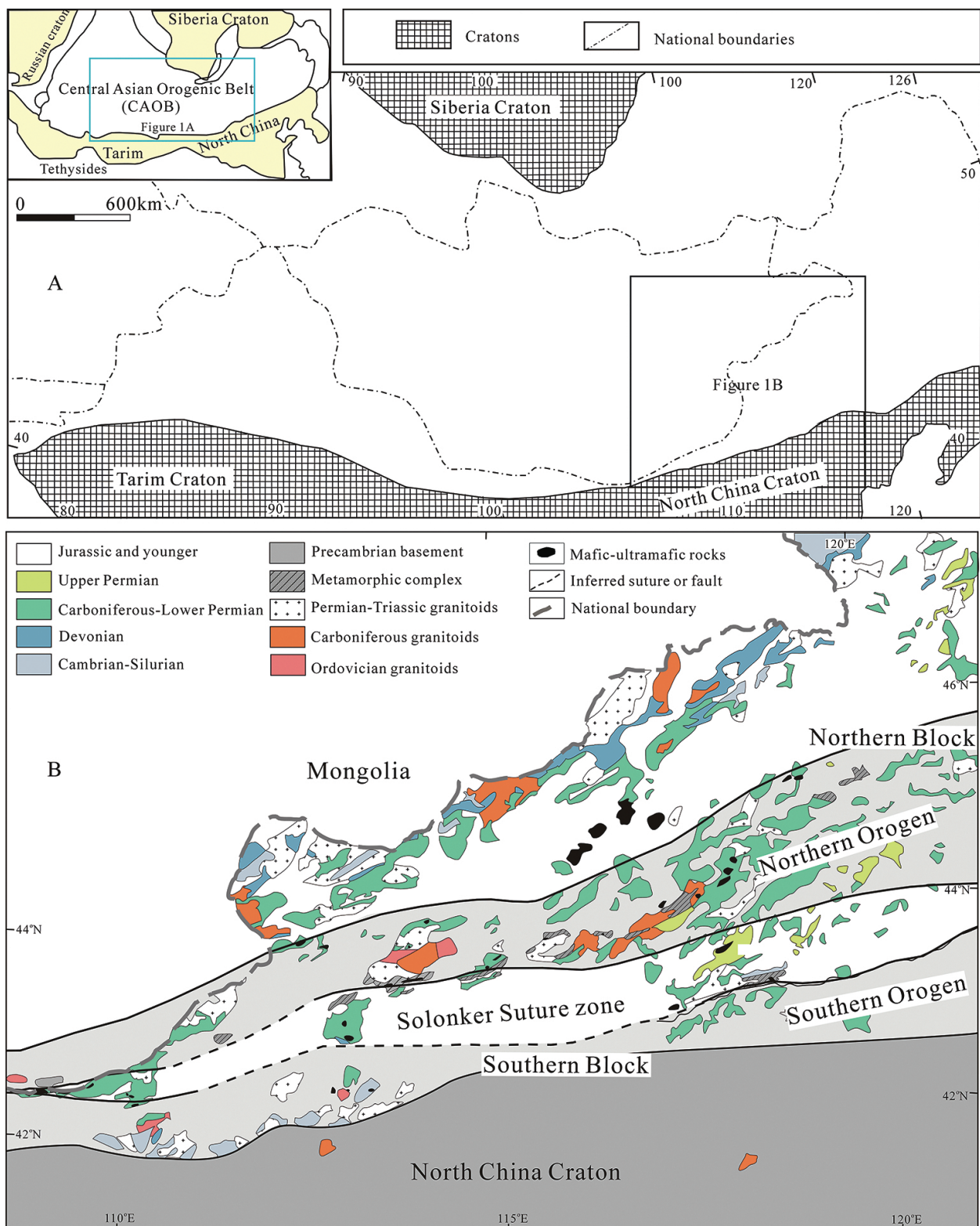


**Figure 1.** Geological sketch map of the southeastern CAOB (the inset map of **Figure 1A** compiled after [19]; **Figure 1B** after [3, 25]). In **Figure 1B**, the Solonker suture zone represents the tectonic boundary between the northern and the southern continental blocks [3].

Paleozoic volcanic rocks and granitoids are widely distributed along the margin of the Solonker suture zone. Ordovician granitoids (quartz-diorite, granodiorite, diorite, tonalite, and trondjemite; **Table 1** and **Figure 2**) occur in the northern and southern orogen [7, 8, 20, 21, 42, 43]; **Figure 1**), whereas Carboniferous volcanic rocks and granitoids (quartz-diorite, granodiorite, tonalite, and granite; **Table 1** and **Figure 2**) are mainly distributed in the northern orogen ([2, 23, 30, 31, 35, 37, 38, 40, 41]; **Figure 1**), and scattered along the northern margin of the North China Craton [44, 45]. The geochemical data of representative rocks are listed in **Table 2**.

Unit	Episode	Lithology	Zircon age (Ma)	Method	$\epsilon_{Hf(t)}$ (Zircon)	$\epsilon_{Nd(t)}$ (Whole rock)	Initial $^{87}Sr/^{86}Sr$ (whole rock)	Reference
Northern Orogen	Ordovician	Quartz diorite	490 ± 8	SHRIMP				[23]
		Tonalite	479 ± 8	SHRIMP		+1.5	0.7053	[7]
		Quartz diorite	475 ± 6	SHRIMP				[7]
		Granodiorite	472 ± 3	SHRIMP	+7.4 to +10.7	+2.2	0.7060	This study
	Carboniferous	Tonalite	464 ± 8	SHRIMP		+1.4	0.7053	[7]
		Tonalite	329 ± 3	SHRIMP		+5.1	0.7043	This study
		Quartz diorite	325 ± 3	SHRIMP				[30]
		Quartz diorite	323 ± 4	SHRIMP				[31]
		Quartz diorite	322 ± 3	SHRIMP				[30]
		Monzogranite	322 ± 1	LA-ICP-MS	+10.6 to +14.0			[32]
		Quartz diorite	320 ± 3	SHRIMP	+8.1 to +12.3	+2.1	0.7051	This study
		Granodiorite	320 ± 8	SHRIMP		+1.0	0.7055	This study
		Andesite	320 ± 7	SHRIMP				[33]
		Granite	319 ± 4	LA-ICP-MS				[34]
		Granodiorite	319 ± 3	SHRIMP				[35]
		Basalt	318 ± 3	LA-ICP-MS				[4]
		Granite	317 ± 2	LA-ICP-MS				[36]
		Garnet bearing granite	316 ± 3	SHRIMP				[29]
		Granodiorite	316 ± 1	LA-ICP-MS	+3.0 to +12.6			[32]
		Quartz diorite	315 ± 4	SHRIMP				[31]
Basalt	315 ± 4	LA-ICP-MS				[4]		
Monzonitic granite	314 ± 2	LA-ICP-MS				[37]		
Quartz diorite	313 ± 5	SHRIMP				[31]		
Granodiorite	312 ± 1	LA-ICP-MS				[38]		

Unit	Episode	Lithology	Zircon age (Ma)	Method	$\epsilon_{Hf(t)}$ (Zircon)	$\epsilon_{Nd(t)}$ (Whole rock)	Initial $^{87}\text{Sr}/^{86}\text{Sr}$ (whole rock)	Reference
Mongolia Hutag Uul		Monzonitic diorite	312 ± 4	SHRIMP				[39]
		Diorite	311 ± 2	SHRIMP				[35]
		Gabbroic diorite	310 ± 5	SHRIMP	+5.4 to +11.5	+2.5	0.7052	[2]
		Quartz diorite	310 ± 2	SHRIMP				[35]
		Volcanic rock	310 ± 1	LA-ICP-MS				[38]
		Quartz diorite	309 ± 8	SHRIMP		-0.2	0.7056	[23]
		Volcanic rock	309 ± 2	LA-ICP-MS				[40]
		Monzonitic granite	308 ± 2	LA-ICP-MS				[36]
		Monzonitic granite	307 ± 2	SHRIMP				[41]
		Volcanic rock	307 ± 6	LA-ICP-MS				[40]
		Rhyolite	303 ± 6	SHRIMP				[33]
		Gneissic granite	1784 ± 7	SHRIMP				Shi et al., unpublished
		Granodiorite	454 ± 10	SHRIMP				Shi et al., unpublished
Southern Orogen	Ordovician	Tonalite	491 ± 8	SHRIMP		+5.2	0.7047	[8]
		Diorite	472					[42]
		Dacite	459 ± 8	SHRIMP				[43]
		Dacite	458 ± 3	SHRIMP		+7.1	0.7058	[8]
		Quartz diorite	454 ± 4	SHRIMP		+2.0	0.7056	[8]
		Diorite	452 ± 3	SHRIMP				[8]
		Trondjemite	451 ± 7	SHRIMP				[43]
		Granodiorite	450					[42]
Northern margin of NCC	Carboniferous	Biotite K-feldspar granite	342 ± 5	SHRIMP				[44]
		Quartz diorite	324 ± 6	SHRIMP				[45]
		Quartz diorite	311 ± 2	SHRIMP				[45]
		Granodiorite	310 ± 5	SHRIMP				[45]
		Quartz diorite	302 ± 4	SHRIMP				[45]
Ophiolitic block								
Erlianhot-Hegenshan		Gabbro	354 ± 7	SHRIMP		+9.8	0.7043	[3]
		Gabbro	298 ± 9	SHRIMP		+8.1	0.7037	[25]
Jiaoqier-		Gabbro	483 ± 2	SHRIMP				[8]

Unit	Episode	Lithology	Zircon age (Ma)	Method	$\epsilon_{Hf(t)}$ (Zircon)	$\epsilon_{Nd(t)}$ (Whole rock)	Initial $^{87}Sr/^{86}Sr$ (whole rock)	Reference
Xilinhot								
Solonker-Linxi		Trondjemite	$324 \pm 3$	SHRIMP		+8.4	0.7039	[3]
		Plagiogranite	$288 \pm 6$	SHRIMP		+7.8	0.7039	[3]
		Gabbro	$284 \pm 4$	SHRIMP		+6.8	0.7043	[3]
Wenduermiao-Xar Moron		Gabbro	$480 \pm 3$	SHRIMP		+9.2	0.7059	[8]

**Table 1.** Summary of zircon ages, Hf isotopic data and whole-rock Sr-Nd isotopic data.

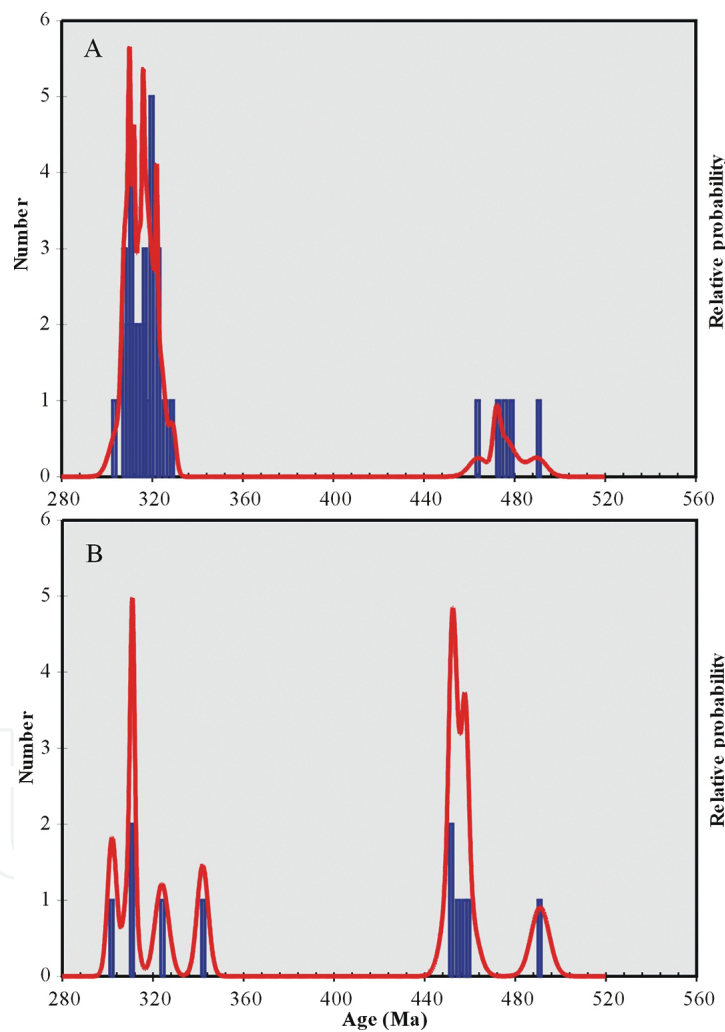


**Figure 2.** Cumulative plot for zircon U-Pb ages of Ordovician and Carboniferous rocks from Central Inner Mongolia (data and references are in Table 1). A for rocks from the Northern Block, which consists of the Southern Mongolia (or Hutag Uul) block and the northern orogen; and B for rocks from the Southern Block, which is composed of the northern margin of North China Craton and the southern orogen [3].

Sample	MS02-7	MB1-3	MS3-5	MB1-6	MB1-1	MB1-5	MB1-2	MB1-4
Lithology	Tonalite	Granodiorite	Tonalite	Tonalite	Granodiorite	Quartz-diorite	Granite	Granite
Age (Ma)	479 ± 8	472 ± 3	464 ± 8	329 ± 3	ca. 320	320 ± 3	297 ± 2	--
SiO <sub>2</sub>	61.13	67.37	61.62	61.98	66.47	54.96	75.19	71.94
TiO <sub>2</sub>	0.42	0.25	0.41	0.59	0.43	0.68	0.18	0.17
Al <sub>2</sub> O <sub>3</sub>	17.05	16.31	16.56	16.22	15.63	18.80	13.76	15.68
TFe <sub>2</sub> O <sub>3</sub>	5.88	3.68	5.62	5.82	4.17	7.98	1.92	1.30
MnO	0.14	0.08	0.14	0.08	0.06	0.12	0.02	0.02
MgO	2.34	1.14	2.27	2.95	1.69	3.65	0.70	0.47
CaO	5.69	3.91	5.78	4.93	3.43	6.25	0.39	1.54
Na <sub>2</sub> O	3.56	4.26	3.08	3.22	3.37	3.14	3.92	5.47
K <sub>2</sub> O	1.34	1.37	1.74	1.49	2.86	0.89	2.62	2.89
P <sub>2</sub> O <sub>5</sub>	0.19	0.12	0.18	0.16	0.14	0.22	0.09	0.11
LOI	1.84	1.40	2.78	2.48	1.81	2.95	1.32	0.73
TOTAL	99.58	99.89	100.18	99.92	100.06	99.64	100.11	100.32
Na <sub>2</sub> O/K <sub>2</sub> O	2.66	3.11	1.77	2.16	1.18	3.53	1.50	1.89
Sc	12.8	5.60	13.4	17.1	9.5	20.0	2.69	0.60
V	115	64	107	123	83	151	33.9	25.1
Cr	20.44	5.0	79.5	45	21	26	8.8	8.1
Co	12.1	6.0	10.6	17.3	10.7	21.8	3.23	2.80
Ni	10.3	3.6	18	29.1	11.4	19.8	7.0	3.9
Cu	5.4	9.1	6.2	38.7	10.3	51.4	23.0	15.8
Zn	51.5	39.2	49.5	55.9	42.7	87.8	18.3	30.9
Ga	16.5	17.4	16.3	16.9	16.1	19.4	12.7	18.1
Ge	1.38	1.48	1.42	1.45	1.17	1.28	1.21	0.78
Rb	32.26	51.1	42.09	69.08	96.9	24.05	99.6	66.5
Sr	649	711	604	304	373	473	198	581
Zr	84.8	78.3	81.9	149.4	171	52.6	75.1	104.4

Sample	MS02-7	MB1-3	MS3-5	MB1-6	MB1-1	MB1-5	MB1-2	MB1-4
Lithology	Tonalite	Granodiorite	Tonalite	Tonalite	Granodiorite	Quartz-diorite	Granite	Granite
Age (Ma)	479 ± 8	472 ± 3	464 ± 8	329 ± 3	ca. 320	320 ± 3	297 ± 2	--
Nb	3.64	4.73	3.2	5.23	6.20	4.96	6.12	1.96
Cs	0.55	0.794	0.8	1.25	1.12	1.54	1.82	1.27
Ba	685.0	471.8	862.4	241.8	687.1	173.8	487.8	511.8
Hf	2.43	2.09	2.43	3.59	4.50	1.33	2.18	2.88
Ta	0.24	0.26	0.23	0.45	0.55	0.25	0.61	0.19
Th	3.78	10.46	2.76	5.83	11.26	0.49	11.83	2.31
U	1	1.48	1.05	1.277	2.16	0.264	0.58	1.11
La	10.92	25.5	7.35	14.67	19.3	9.45	8.91	5.41
Ce	22.7	49.3	17.01	29.3	37.9	20.9	28.4	14.3
Pr	2.85	4.58	2.11	3.78	4.23	2.63	1.97	1.25
Nd	11.85	15.8	9.03	16.2	16.2	11.6	7.12	5.11
Sm	2.67	2.19	2.32	3.63	3.09	2.61	1.33	1.00
Eu	0.84	0.61	0.77	1.00	0.81	0.88	0.32	0.38
Gd	2.57	2.09	2.26	3.84	2.81	2.72	1.45	0.93
Tb	0.42	0.23	0.38	0.64	0.40	0.42	0.22	0.11
Dy	2.39	1.32	2.26	3.77	2.31	2.54	1.46	0.72
Ho	0.52	0.26	0.51	0.87	0.48	0.53	0.33	0.12
Er	1.52	0.78	1.39	2.32	1.29	1.41	0.95	0.35
Tm	0.25	0.12	0.23	0.39	0.20	0.22	0.16	0.038
Yb	1.64	0.95	1.61	2.61	1.42	1.50	1.18	0.37
Lu	0.27	0.15	0.28	0.44	0.24	0.24	0.18	0.028
Y	16.2	9.1	14.5	27.0	14.1	16.9	11.1	4.68
La/Yb	6.7	26.8	4.6	5.6	13.6	6.3	7.6	14.6
Sr/Y	40	78	42	11	27	28	18	124

**Table 2.** Major oxide (wt.%) and trace element (ppm) composition of representative samples.

**Figure 3** shows the photographs of field occurrences and photomicrographs of some representative samples. **Figure 3A** was taken from Central Inner Mongolia to show the beautiful landscape; **Figure 3B** shows the Carboniferous volcanic rocks which are located in the Southern Block.

Granodiorite sample MB1-3 (**Figure 3C** and **3D**), collected from Baiyinbaolidao, southern Sonidzuqi, which is located in the Northern Block, is medium-grained, foliated and consists of plagioclase (45–50 vol.%), quartz (20–25%), K-feldspar (10–15), biotite (5–10%), hornblende (1–5%), accessory zircon, apatite and sphene. Plagioclase is partially epidotized, sericitized and biotite grains are chloritized.

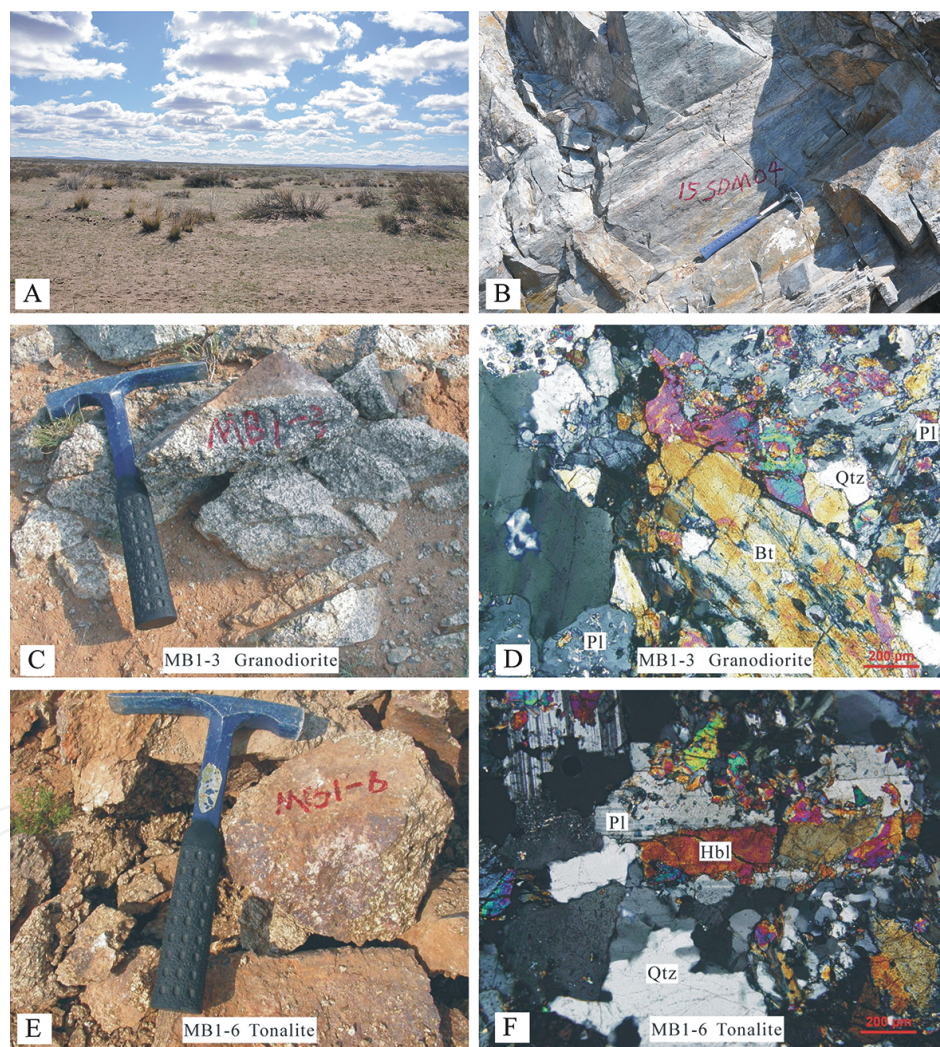


**Figure 3.** Photographs to show field occurrences and photomicrographs of some representative samples.

Tonalite sample MB1-6 (**Figure 3E** and **3F**), which is also collected from Baiyinbaolidao, Southern Sonidzuqi, is medium-grained and consists of plagioclase (60–65%), quartz (20–25%), hornblende (10–15%) and biotite (1–5%) with trace amounts of zircon, apatite and sphene. Plagioclase is partially epidotized, and biotite grains are chloritized.

### 3. Petrogenesis of the Ordovician and Carboniferous volcanic rocks and granitoids

The Ordovician granitoid samples have intermediate to high-silica (61.13–67.37 wt.%), high  $\text{Al}_2\text{O}_3$  (mostly >15 %), higher  $\text{Na}_2\text{O}$  than  $\text{K}_2\text{O}$  ( $\text{Na}_2\text{O} > \text{K}_2\text{O}$ ,  $\text{Na}_2\text{O}/\text{K}_2\text{O} = 1.77\text{--}3.11$ ), low  $\text{MgO}$  (<3%), low HREE (**Figure 4**), depleted HFSE (**Figure 5**), Y and Yb ( $\text{Y} < 18$  ppm,  $\text{Yb} < 1.9$  ppm), high Sr (604–711 ppm), Sr/Y mostly >40 (40.1–78.1) (**Table 2**; **Figure 6**) and low  $I_{\text{Sr}}$  with positive  $\varepsilon_{\text{Nd}}(t)$  isotope ratios (**Table 1**; **Figure 7**). The Ordovician granitoid samples therefore represent adakitic compositions ([16, 48]; **Table 3**).

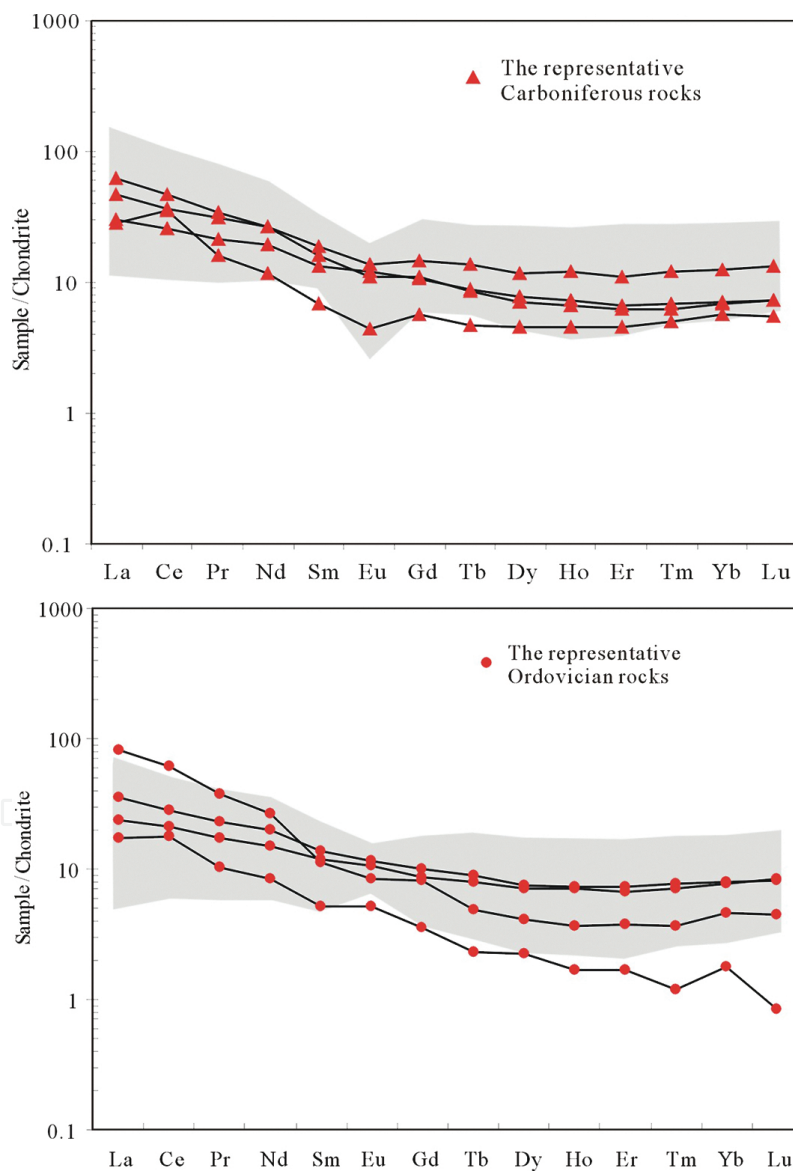


**Figure 4.** Chondrite (CHON)-normalized REE patterns for representative samples (grey fields show data from [7, 8, 43] for Ordovician granitoids; and from [23, 30, 32, 34, 36, 37] for Carboniferous granitoids). Chondrite values are from [46].

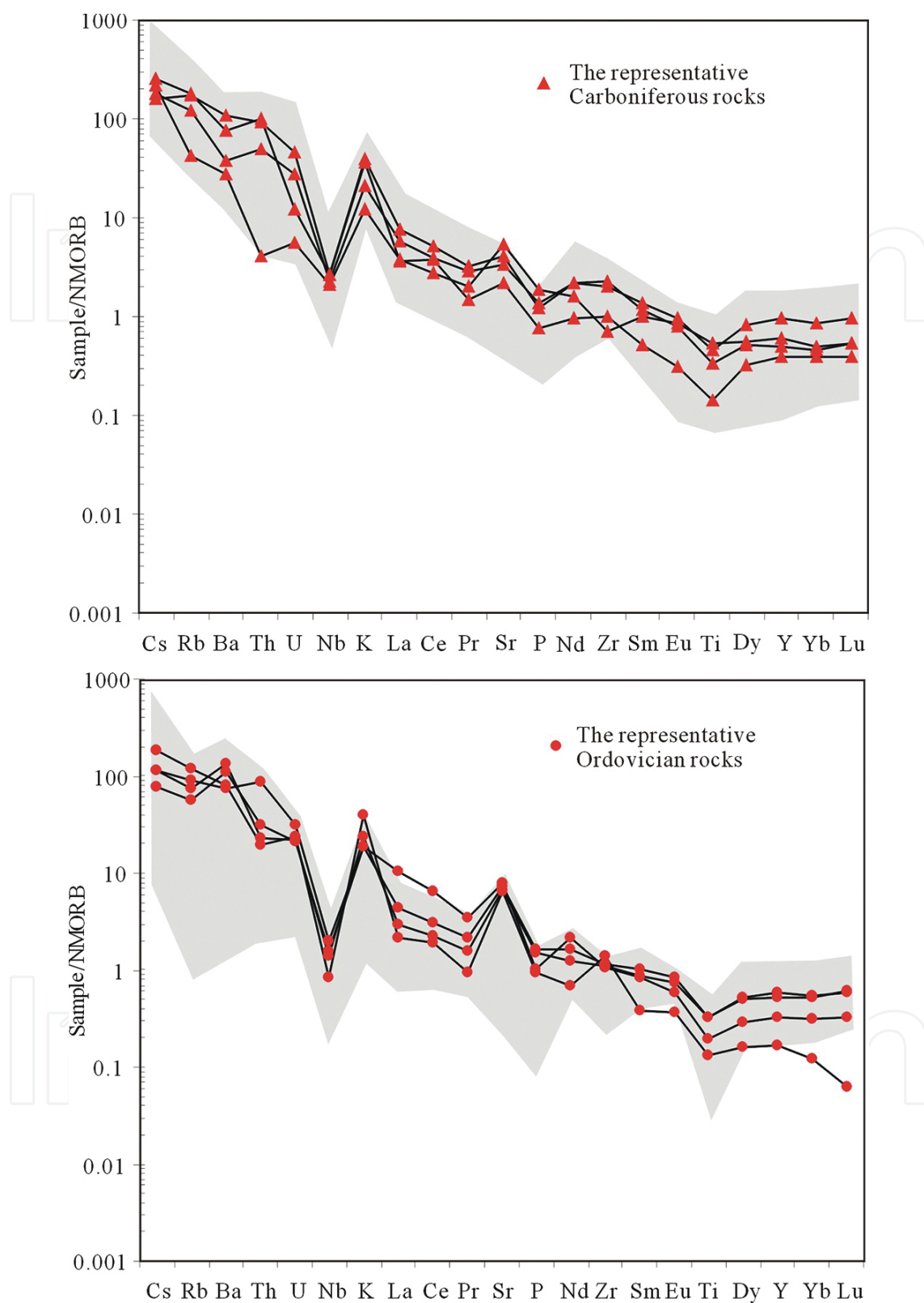


**Figure 5.** N-MORB-normalized trace element variation diagrams for representative samples (grey fields show data from [7, 8, 43] for Ordovician granitoids; and from [23, 30, 32, 34, 36, 37] for Carboniferous granitoids). N-MORB values are from [47].

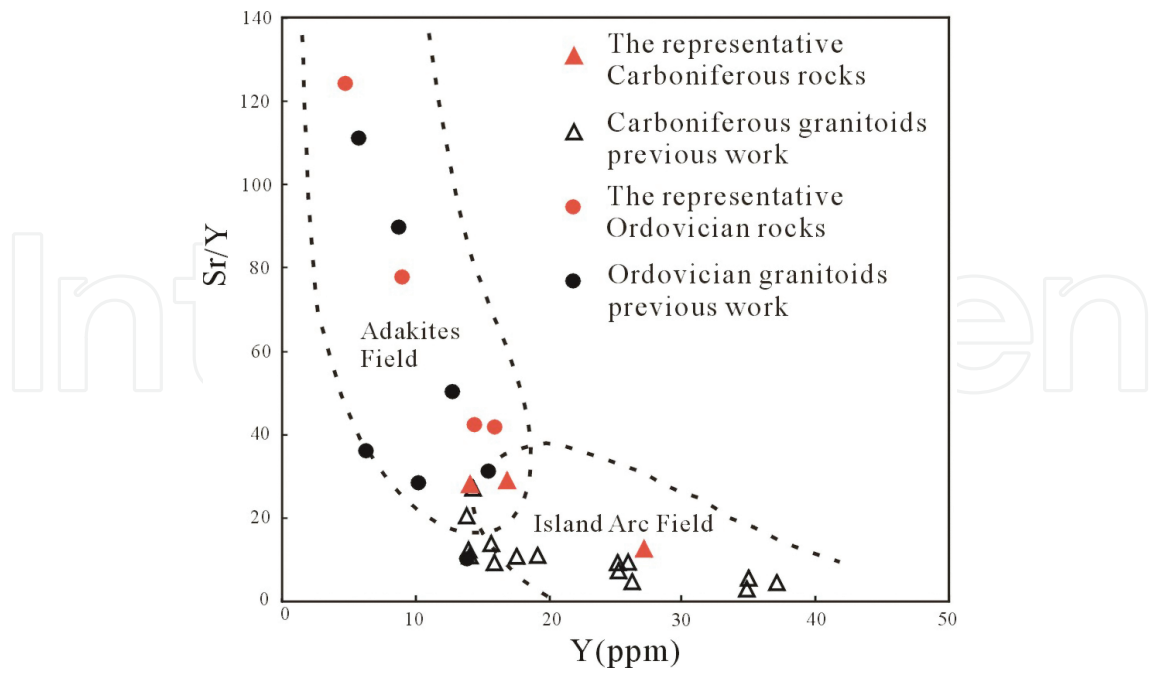


**Figure 6.** Y vs. Sr/Y plot showing adakitic rocks (after [18]) (data from [7, 8, 43] for Ordovician rocks; and from [23, 30, 32, 34, 36, 37] for Carboniferous rocks).

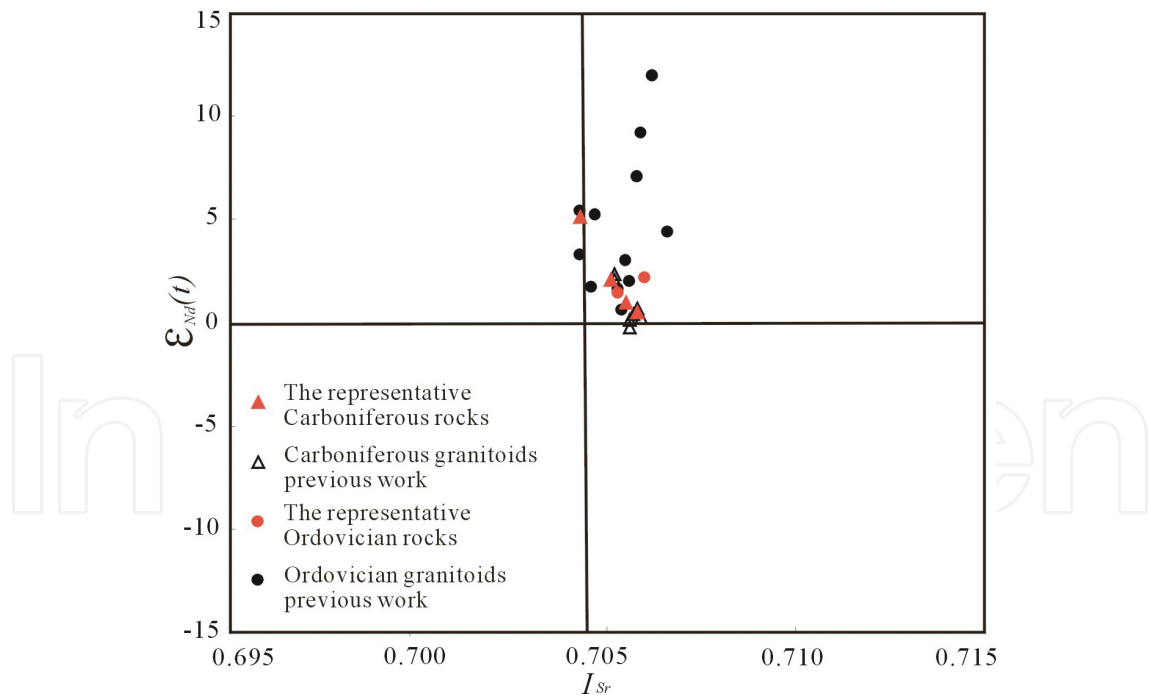


**Figure 7.**  $I_{Sr}$  vs.  $\epsilon_{Nd(t)}$  for some typical Ordovician and Carboniferous rocks with high Sr/Y ratio from Central Inner Mongolia (data from [8, 23]).

	Ada kites	Cook island <sup>b</sup>	Cerro Pampa <sup>c</sup>	MS02-7MB1-3 Tona lite	MS3-5Oceanic Grano diorite	Tona lite	arc granites	Oman <sup>d</sup>	Little Port <sup>d</sup>	Jamaica <sup>d</sup>	Chile <sup>d</sup>	Active continental margin arc granites	MB1-6MB1-1 Tona arc lite	MB1-5 Quartz- diorite
SiO <sub>2</sub> (%)	≥56.0	61.4	62.6	61.13	67.37	61.62	70.1	69.5	68.4	74.5	61.98	66.47	54.96	
Al <sub>2</sub> O <sub>3</sub> (%)	≥15.0	18.4	17.3	17.05	15.68	16.56	12.0	14.60	14.44	12.52	16.22	15.63	18.80	
Na <sub>2</sub> O /K <sub>2</sub> O	>1.00	7.75	3.82	2.66	3.11	1.77	15.75	4.37	1.18	0.65	2.16	1.18	3.53	
MgO (%)	<3			2.34	1.14	2.27					2.95	1.69	3.65	
Y (μg/g)	≤18.00	6		16.2	9.1	14.5	44	19	10	30	27.0	14.1	16.9	
Yb (μg/g)	≤1.90	0.85	0.72	1.64	0.15	1.61	4.54		1.37	3.12	2.61	1.42	1.50	
Sr (μg/g)	>400	1910	1886	649	711	604	200	274	210	93	304	373	473	
Sr/Y	>20	319		40	78	42	4.6	14.4	21.0	3.1	11	26	28	
Sr ano maly	Posi tive	Posi tive		Posi tive	Posi tive	Posi tive					Posi tive	Posi tive	Posi tive	
Eu no maly	Posi tive or weakly nega tive			Weakly nega tive	Nega tive	Posi tive					Nega tive	Nega tive	Weakly posi tive	
Age (Ma)	<25 Ma	<24 Ma	ca. 12 Ma	479 ± 8	472 ± 3	464 ± 8					329 ± 3	ca. 320	320 ± 3	

<sup>a</sup> [16, 49].

<sup>b</sup> Cook island adakites [50].

<sup>c</sup> Cerro Pampa adakites [51].

<sup>d</sup> [52].

**Table 3.** The comparison of geochemical characteristics between the rocks from Central Inner Mongolia, the typical adakitic and arc rocks.

The genesis of adakites is extensively debated, and there are four proposed origins, namely partial melting of young subducted lithosphere [16], melting of newly underplated lower continental crust [53], differentiation of a parental basaltic magma [54, 55] and melting of foundered mafic lower continental crust [56]. High-Al, high  $\text{Na}_2\text{O}$  and calc-alkaline adakites are generally interpreted to have formed due to the melting of subducted oceanic crust and are different from high-K, high total alkali ( $\text{Na}_2\text{O} + \text{K}_2\text{O}$ ) and low  $\text{Al}_2\text{O}_3$  adakites that form through melting of thickened basaltic lower continental crust [16, 51, 53, 57–60].

The Inner Mongolian Ordovician granitoids of this study have depleted HREE, Nb, positive Sr anomalies, low Y and Yb contents and positive to weakly negative Eu anomalies. These characteristics are consistent with the loss of plagioclase and the presence of garnet as residual phases, probably related to partial melting of the source material under eclogite-facies conditions [61, 62]. The petrology and geochemistry of the Ordovician adakitic granitoids indicate a contribution from melting of subducted oceanic crust in their formation rather than melting of thickened basaltic lower continental crust.

The Carboniferous samples in this area have intermediate to high-silica (54.96–66.47 wt.%), high  $\text{Al}_2\text{O}_3$  (15.63–18.80 %), higher  $\text{Na}_2\text{O}$  than  $\text{K}_2\text{O}$  ( $\text{Na}_2\text{O} > \text{K}_2\text{O}$ ,  $\text{Na}_2\text{O}/\text{K}_2\text{O} = 1.18\text{--}3.53$ ), low HREE (**Table 2; Figure 4**), and with low  $I_{\text{Sr}}$  (0.7043–0.7060), positive  $\varepsilon_{\text{Nd}}(t)$  (+1.0 to +5.1) and  $\varepsilon_{\text{Hf}}(t)$  (+8.1 to +12.3) isotope ratios (**Table 1; Figures 7 and 8**). However, most of them have lower Sr and Sr/Y ratio than those of Ordovician adakitic granitoids in this area (**Table 2; Figure 6**), which are typical subduction-related arc granitoids [52, 63, 64] although still with adakite-like compositions [16, 48].

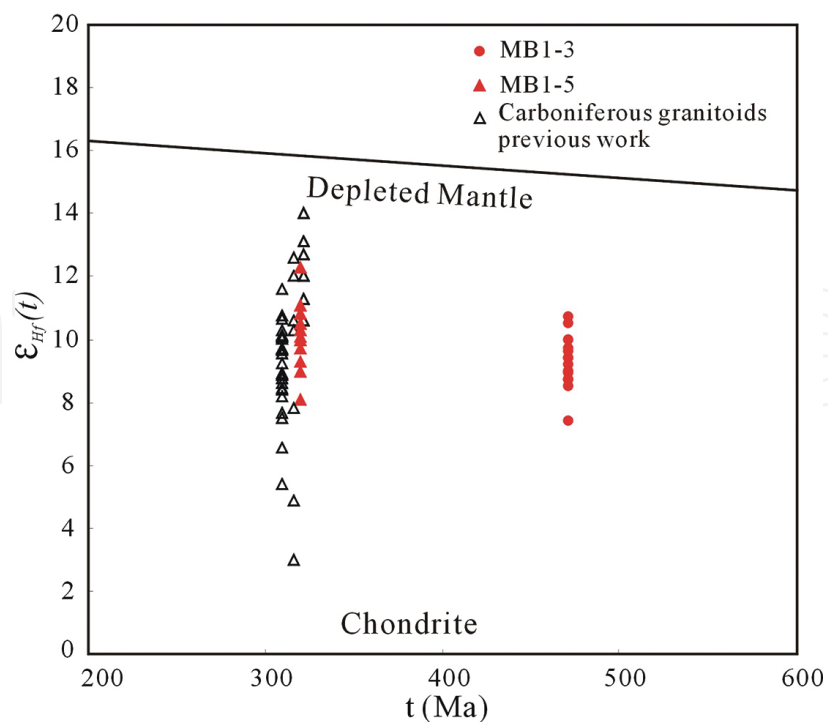


**Figure 8.** U-Pb age vs.  $\varepsilon_{\text{Hf}}(t)$  for zircons from (data from [2], and [32] for Carboniferous granitoids).

#### 4. Geodynamic significance of the Ordovician and Carboniferous volcanic rocks and granitoids

A subduction-accretion complex usually forms along a convergent plate boundary where an oceanic plate subducts beneath another oceanic or continental plate [65]. Early Paleozoic arc plutonism as part of trench-island arc-basin systems ([6, 8, 21, 22]; **Table 2**) occurred in the southern orogen, along the northern margin of the North China Craton, and late Silurian molasse deposits unconformably overlie these rocks [6, 66]. Coeval adakitic plutonism is emplaced in the northern orogen, along the southern margin of the Mongolian terrane [20]. Silurian high-pressure metamorphic rocks [67] and Silurian syncollisional magmatism in the northern orogen along the Solonker suture [68] were also reported. All these features indicate an early-middle Paleozoic subduction and accretion system along the northern margin of the North China Craton and the southern margin of the Mongolian terrane. After demise of the ocean in the southern orogen, caused by subduction of a ridge crest and by ridge collision with supra-subduction zone ophiolite in the Silurian [8], the southern orogen became tectonically consolidated and turned into a post-orogenic setting [69].

There has been some debate about whether the Carboniferous calc-alkaline granitoids formed in a subduction zone [23, 30] or in a late- to post-orogenic setting [31]. Carboniferous calc-alkaline plutonic rocks (ca. 328–308 Ma) in the northern orogen were suggested by [2, 23, 30] as subduction genesis, which can be related to the northward subduction of Asian ocean slab. Bao et al. [31], however, thought these Carboniferous granitoids formed in a Late Paleozoic rift area because of Permian bimodal volcanic rocks. These Carboniferous granitoids include variably foliated gabbro, diorite, quartz diorite, granodiorite, tonalite and granite [23, 30], which belong to low-K tholeiitic and calc-alkaline series, and are enriched in large ion lithophile elements (LILE) and depleted in high field strength elements (HFSE) [2, 23, 30], low  $I_{Sr}$ , positive  $\varepsilon_{Nd}(t)$  and  $\varepsilon_{Hf}(t)$  isotope ratios ([23]) showing subduction-related arc granitoids characteristics [52, 63, 64].

Additionally, a subduction-accretion complex was identified from previously defined late Carboniferous and early Permian strata in the Daqing pasture, southern Xiwuqi, Inner Mongolia [4]. In addition to this subduction-accretion complex, most magmatic rocks are considered to have formed in a subduction setting [23, 30], and the spatial configuration of both geological units indicates that the subduction polarity was from south to north [4] along the northern orogen.

Carboniferous granitoids on the northern margin of North China craton also have the composition of tholeiitic and calc-alkaline island-arc rocks and adakitic compositions [45], however, low negative whole-rock  $\varepsilon_{Nd}(t)$  and zircon  $\varepsilon_{Hf}(t)$  isotope ratios indicate that they were derived mainly from anatectic melting of the ancient lower crust with some involvement of mantle materials [70]. The Carboniferous plutons were interpreted as subduction-related and emplaced in an Andean-style continental-margin arc [70].

On the northern margin of the North China craton, however, Carboniferous eclogites are exposed at least 200 km south of the Solonker suture zone and have tholeiitic protoliths (MORB

and IAT), and eclogite-facies metamorphism reflects deep subduction of oceanic lithosphere [71]. The granitoids (330–298 Ma) of this area were emplaced and deformed during, and/or shortly after eclogite-facies metamorphism (ca. 331–319 Ma) [71]. This close temporal relationship indicates that magmatism closely followed the exhumation of the high-pressure metamorphic terrane [3].

## 5. A possible model for the discrete evolution of CAOB

The southeastern CAOB was formed by the concurrent two-way subduction of Paleo-Central Asian Ocean towards opposing continental margins in the early Paleozoic (**Figure 9A**). In the south is an arc-trench complex, which can be regarded as an analogue of the Izu-Bonin-Mariana arc [72], and in the north a product of ridge-trench interaction [8]. In the late Paleozoic, however, Andean-type orogenesis was induced by subduction of Central Asian Ocean beneath either the northern (e.g. [4]) or southern (e.g. [45]) continental blocks (**Figure 9B**). Plutonic magmatism [45] was accompanied by exhumation of a high-pressure metamorphic terrane [71] in the south; and a subduction-accretion complex [4], together with most arc-related magmatic rocks [23, 30] was formed along the northern orogen.

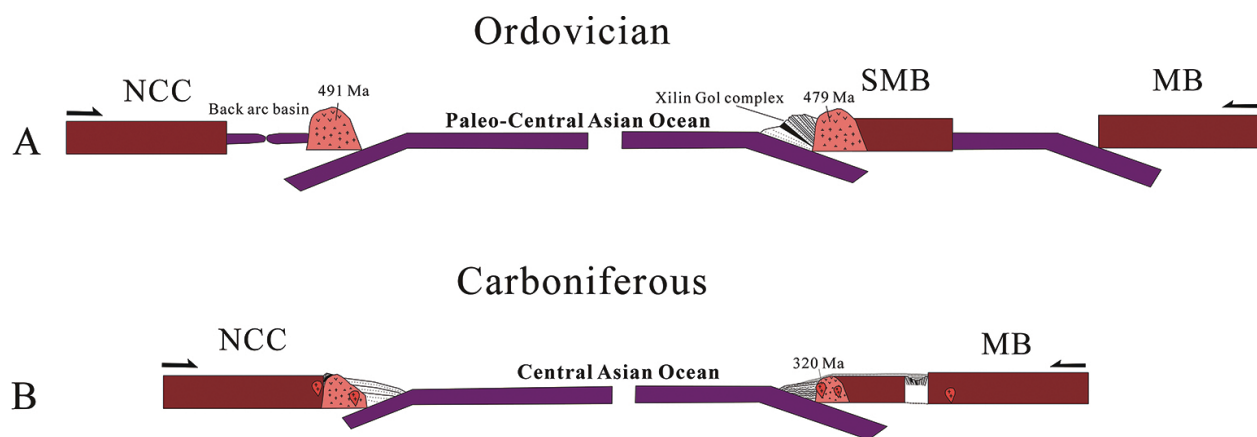


**Figure 9.** A possible model for Ordovician and Carboniferous evolution of Central Inner Mongolia. Abbreviation: NCC, North China Craton; SMB, South Mongolia Block; MB, Mongolia Block.

## 6. Modern equivalent

### 6.1. Cook Island and Cerro Pampa adakites

Cenozoic andesitic to dacitic rocks collected from Cerro Pampa [51] and andesites from Cook Island [50] have intermediate to high-silica, high  $\text{Al}_2\text{O}_3$ , higher  $\text{Na}_2\text{O}$  than  $\text{K}_2\text{O}$ , low HREE,

depleted HFSE, Y and Yb, high Sr, and high Sr/Y ratios (**Table 3**), and low  $I_{Sr}$  with positive  $\epsilon_{Nd}$  isotope ratios. The samples, therefore, represent adakites [50, 51]. Cerro Pampa adakitic magmas formed in response to melting of hot slab that was subducting beneath South America [51], and similar petrogenesis for the Austral Volcanic Zone adakites [50]. Ordovician adakitic rocks from Central Inner Mongolia show similar petrogenesis and geotectonic setting with the Cenozoic adakites from Cook Island [50], Cerro Pampa [51] and Aleutian arc [16].

## 6.2. Oman and Chile volcanic arc granites

Volcanic arc granites from Oman and Chile have high-silica, intermediate  $Al_2O_3$ , low HREE [52] (**Table 3**), and with low Sr and Sr/Y ratios than the adakites (**Table 3**), which are typical subduction-related arc granitoids derived from melting in the mantle wedge. Most Carboniferous volcanic rocks and granitoids present similar petrogenesis and geotectonic setting with the Cenozoic subduction-related arc granitoids.

## 7. Conclusions

1. The Ordovician and Carboniferous volcanic rocks and granitoids are mostly intermediate to high-silica, high  $Na_2O/K_2O$  ratio, high Sr/Y ratios. They are characterized by LREE enrichment and exhibit typical negative Nb anomalies. All samples show positive  $\epsilon_{Hf}(t)$ ,  $\epsilon_{Nd}(t)$  values and low  $I_{Sr}$ .
2. The Ordovician rocks show higher Sr/Y ratio than the Carboniferous rocks, suggesting that the former represent adakitic rocks and the latter are typical subduction-related arc rocks with adakite-like compositions.
3. The Central Asian Orogenic Belt evolved through several subduction systems with different polarities in Central Inner Mongolia, namely an early-middle Paleozoic subduction and accretion system along the northern margin of the North China Craton and the southern margin of the Mongolian terrane, and late Paleozoic northward subduction along the northern orogen and exhumation of a high-pressure metamorphic terrane on the northern margin of the North China Craton.

## Acknowledgements

The editorial patience and the comments of Dr. Karoly Nemeth are appreciated. This study was financially supported by the National Natural Science Foundation of China (Grant nos. 40703012) and Geological Survey of China (Grant nos. 1212011121075, 12120114020901, 12120114064301, and 1212011120332).

## Author details

Yuruo Shi

Address all correspondence to: shiyuruo@bjshrimp.cn

Beijing SHRIMP Center, Institute of Geology, Chinese Academy of Geological Sciences, Beijing, China

## References

- [1] Xiao W.J., Windley B.F., Hao J., Zhai M.G., 2003. Accretion leading to collision and the Permian Solonker suture, Inner Mongolia, China: termination of the Central Asian orogenic belt. *Tectonics* 22, 8–20.
- [2] Chen B., Jahn B.M., Tian W., 2009. Evolution of the Solonker suture zone: constraints from zircon U-Pb ages, Hf isotopic ratios and whole-rock Nd-Sr isotope compositions of subduction- and collision-related magmas and forearc sediments. *Journal of Asian Earth Sciences* 34, 245–257.
- [3] Jian P., Liu D.Y., Kröner A., Windley B.F., Shi Y.R., Zhang W., Zhang F.Q., Miao L.C., Zhang L.Q., Tomurhuu D., 2010. Evolution of a Permian intraoceanic arc-trench system in the Solonker suture zone, Central Asian Orogenic Belt, China and Mongolia. *Lithos* 118(1), 169–190.
- [4] Liu J.F., Li J.Y., Chi X.G., Qu J.F., Hu Z.C., Fang S., Zhang Z., 2013. A late-Carboniferous to early early-Permian subduction-accretion complex in Daqing pasture, southeastern Inner Mongolia: evidence of northward subduction beneath the Siberian paleoplate southern margin. *Lithos* 177, 285–296.
- [5] Shi Y.R., Liu C., Deng J.F., Jian P., 2014. Geochronological frame of granitoids from Central Inner Mongolia and its tectonomagmatic evolution. *Acta Petrologica Sinica* 30 (11), 3155–3171 (in Chinese with English abstract).
- [6] Tang K.D., 1990. Tectonic development of Paleozoic foldbelts at the north margin of the Sino-Korean craton. *Tectonics* 9, 249–260.
- [7] Shi Y.R., Liu D.Y., Zhang Q., Jian P., Zhang F.Q., Miao L.C., Shi G.H., Zhang L.Q., Tao H., 2004. SHRIMP dating of diorites and granites in southern Suzuoqi, Inner Mongolia. *Acta Geologica Sinica* 78(6), 789–799. (in Chinese with English abstract).
- [8] Jian P., Liu D.Y., Kröner A., Windley B.F., Shi Y.R., Zhang F.Q., Shi G.H., Miao L.C., Zhang W., Zhang Q., 2008. Time scale of an early to mid-Paleozoic orogenic cycle of the long-lived Central Asian Orogenic Belt, Inner Mongolia of China: Implications for continental growth. *Lithos* 101, 233–259.

- [9] Xu B., Zhao P., Wang Y.Y., Liao W., Luo Z.W., Bao Q.Z., Zhou Y.H., 2015. The pre-Devonian tectonic framework of Xing'an-Mongolia orogenic belt (XMOB) in north China. *Journal of Asian Earth Sciences* 97, 183–196.
- [10] Sengör A.M.C., Natal'in B.A., Burtman V.S., 1993. Evolution of the Altaid tectonic collage and Paleozoic crustal growth in Eurasia. *Nature* 364, 299–307.
- [11] Coleman R.G., 1989. Continental growth of Northwest China. *Tectonics* 8, 621–635.
- [12] Mossakovskii A.A., Ruzhentsev S.V., Samygin S.G., Kheraskova T.N., 1993. Central Asian Foldbelt: geodynamic evolution and formation history. *Geotektonika* 6, 3–32 (in Russian).
- [13] Kröner A., Windley B.F., Badarch G., Tomurtogoo O., Hegner E., Jahn B.M., Gruschka S., Khain E.V., Demoux A., Wingate M.T.D., 2007. Accretionary growth and crust formation in the Central Asian Orogenic Belt and comparison with the Arabian-Nubian-Shield. *Geological Society of America, Memorials* 200, 181–209.
- [14] Kröner A., Kovach V., Belousova E., Hegner E., Armstrong R., Dolgoplova A., Seltmann R., Alexeiev D.V., Hoffmann J.E., Wong J., Sun M., Cai K., Wang T., Tong Y., Wilde S.A., Degtyarev K.E., Ryt'sk E., 2014. Reassessment of continental growth during the accretionary history of the Central Asian Orogenic Belt. *Gondwana Research* 25, 103–125.
- [15] Windley B.F., Alexeiev D., Xiao W.J., Kröner A., Badarch G., 2007. Tectonic models for accretion of the Central Asian Orogenic Belt. *Journal of the Geological Society* 164 (1), 31–47.
- [16] Defant M.J., Drummond M.S. 1990. Derivation of some modern arc magmas by melting of young subducted lithosphere. *Nature* 347, 662–665.
- [17] Gill J.B., 1981. *Orogenic Andesites and Plate Tectonics*. Springer, Berlin.
- [18] Defant M.J., Drummond M.S., 1993. Mount St. Helens: potential example of the partial melting of the subducted lithosphere in a volcanic arc. *Geology* 21(6), 547–550.
- [19] Jahn B.M., Wu F.Y., Chen B., 2000. Granitoids of the Central Asian Orogenic Belt and continental growth in the Phanerozoic. *Transactions Royal Society of Edinburgh: Earth Sciences* 91, 181–193.
- [20] Shi Y.R., Liu D.Y., Zhang Q., Jian P., Zhang F.Q., Miao L.C., Shi G.H., Zhang L.Q., Tao H., 2005a. The petrogenesis and SHRIMP dating of the Baiyinbaolidao adakitic rocks in south Suzuqi, Inner Mongolia. *Acta Petrologica Sinica* 21, 143–150 (in Chinese with English abstract).
- [21] Zhang W., Jian P., 2008. SHRIMP dating of Early Paleozoic granites from North Damaoqi, Inner Mongolia. *Acta Geologica Sinica* 82, 778–787 (in Chinese with English abstract).

- [22] Zhang W., Jian P., Kröner A., Shi Y.R., 2013. Magmatic and metamorphic development of an early to mid-Paleozoic continental margin arc in the southernmost Central Asian Orogenic Belt, Inner Mongolia, China. *Journal of Asian Earth Sciences* 72, 63–74.
- [23] Chen B., Jahn B.M., Wilde S., Xu B., 2000. Two contrasting Paleozoic magmatic belts in northern Inner Mongolia, China: petrogenesis and tectonic implications. *Tectonophysics* 328, 157–182
- [24] Badarch G., Cunningham W.D., Windley B.F., 2002. A new terrane subdivision for Mongolia: implications for the Phanerozoic crustal growth of Central Asia. *Journal of Asian Earth Sciences* 21 (1), 87–110.
- [25] Miao L.C., Fan W.M., Liu D.Y., Zhang F.Q., Shi Y.R., Guo, F., 2008. Geochronology and geochemistry of the Hegenshan ophiolitic complex: Implications for late-stage tectonic evolution of the Inner Mongolia-Daxinganling Orogenic Belt, China. *Journal of Asian Earth Sciences* 32: 348–370.
- [26] Dobretsov N.L., Berzin N.A., Buslov M.M., 1995. Opening and tectonic evolution of the Paleo-Asian Ocean. *International Geology Review* 37 (4), 335–360.
- [27] Jian P., Shi Y.R., Zhang F.Q., Miao L.C., Zhang L.Q., Kröner A., 2007. Geological excursion to Inner Mongolia, China, to study the accretionary evolution of the southern margin of the Central Asian Orogenic Belt. Structural and tectonic correlation across the Central Asia Orogenic Collage: Implications for continental growth and intracontinental deformation (Abstracts and Excursion guidebook). The Third International workshop and field excursions for IGC Project 480: 49–72.
- [28] Li J.Y., 2006. Permian geodynamic setting of Northeast China and adjacent regions: closure of the Paleo-Asian Ocean and subduction of the Paleo-Pacific Plate. *Journal of Asian Earth Sciences* 26, 207–224.
- [29] Shi G.H., Liu D.Y., Zhang F.Q., Jian P., Miao L.C., Shi Y.R., Tao H., 2003. Zircon SHRIMP U-Pb geochronology and significance of the Xilinhote metamorphic complex, Inner Mongolia, China. *Chinese Science Bulletin* 48(20), 2187–2192 (in Chinese).
- [30] Liu J.F., Chi X.G., Zhang X.Z., Ma Z.H., Zhao Z., Wang T.F., Hu Z.C., Zhao X.Y., 2009. Geochemical characteristic of Carboniferous quartz-diorite in the southern Xiwuqi area, Inner Mongolia and its tectonic significance. *Acta Geologica Sinica* 83 (3), 365–376 (in Chinese with English abstract).
- [31] Bao Q.Z., Zhang C.J., Wu Z.L., Wang H., Li W., Sang J.H., Liu Y.S., 2007. SHRIMP U-Pb zircon geochronology of a Carboniferous quartz-diorite in Baiyingaole area, Inner Mongolia and its implications. *Journal of Jilin University (Earth Science Edition)* 37 (1), 15–23 (in Chinese with English abstract).
- [32] Hu C.S., Li W.B., Xu C., Zhong R.C., Zhu F., 2015. Geochemistry and zircon U-Pb-Hf isotopes of the granitoids of Baolidao and Halatu plutons in Sonidzuoqi area, Inner

- Mongolia: Implications for petrogenesis and geodynamic setting. *Journal of Asian Earth Sciences* 97, 294–306.
- [33] Xin H.T., Teng X.J., Cheng Y.H., 2011. Stratigraphic Subdivision and Isotope Geochronology Study on the Baoligaomiao Formation in the East Ujimqin County, Inner Mongolia. *Geological Survey and Research* 34, 1–8 (in Chinese with English abstract).
- [34] Liang Y.W., Yu C.L., Shen G.Z., Sun Q.R., Li J.W., Yang Y.C., She H.Q., Zhang B., Tan G., 2013. Geochemical characteristics of granites in the Suonaga Pb-Zn-Ag deposit of Dong Ujimqin Banner, Inner Mongolia, and their tectonic and ore-forming implications. *Geology in China* 40, 767–779 (in Chinese with English abstract).
- [35] Xue H.M., Guo L.J., Hou Z.Q., Tong Y., Pan X.F., Zhou X.W., 2010. SHRIMP zircon U-Pb ages of the middle Neopaleozoic unmetamorphosed magmatic rocks in the southwestern slope of the DaHinggan Mountains, Inner Mongolia. *Acta Petrologica et Mineralogica* 29, 811–823 (in Chinese with English abstract).
- [36] Xu L.Q., Ju W.X., Liu C., He H.Y., Li M.Y., 2012. Sr-Yb classification and genesis of late Carboniferous granites in Arenshaobu area of Erenhot, Inner Mongolia. *Geological Bulletin of China* 31, 1410–1419 (in Chinese with English abstract).
- [37] He F.B., Xu J.X., Gu X.D., Cheng X.B., Wei B., Li Z., Liang Y.N., Wang Z.L., Huang Q., 2013. Ages, origin and geological implication of the Amuguleng composite granite in East Ujimqin Banner, Inner Mongolia. *Geological Review* 59, 1150–1164 (in Chinese with English abstract).
- [38] Li K., Zhang Z.C., Feng Z.S., Li J.F., Tang W.H., Luo Z.W., C.Y., 2015. Two-phase magmatic events during late Paleozoic in the north of the Central Inner Mongolia-Da Hinggan orogenic belt and its tectonic significance. *Acta Geologica Sinica* 89, 272–288 (in Chinese with English abstract).
- [39] Yun F., Nie F.J., Jiang S.H., Liu Y., Zhang W.Y., 2011. Zircon SHRIMP U-Pb age of Monuogechin monzodiorite of Inner Mongolia and its geological significance. *Mineral Deposits* 30, 504–510 (in Chinese with English abstract).
- [40] Li K., Zhang Z.C., Feng Z.S., Li J.F., Tang W.H., Luo Z.W., 2014. Zircon SHRIMP U-Pb dating and its geological significance of the Late-Carboniferous to Early-Permian volcanic rocks in Bayanwula area, the central of Inner Mongolia. *Acta Petrologica Sinica* 30, 2041–2054 (in Chinese with English abstract).
- [41] Cheng Y.H., Teng X.J., Xin H.T., Yang J.Q., Ji S.P., Zhang Y., Li Y.F., 2012. SHRIMP zircon U-Pb dating of granites in Mahonondor area, East Ujimqin Banner, Inner Mongolia. *Acta Petrologica et Mineralogica* 31, 323–334 (in Chinese with English abstract).
- [42] Xu L.Q., Deng J.F., Chen Z.Y., Tao J.X. 2003. The identification of Ordovician adakites and its signification in northern Damao, Inner Mongolia. *Geoscience* 17, 428–434 (in Chinese with English abstract).

- [43] Liu D.Y., Jian P., Zhang Q., Zhang F.Q., Shi Y.R., Shi G.H., Zhang F.Q., Tao H., 2003. SHRIMP dating of adakites in the Tulingkai ophiolite, Inner Mongolia: evidence for the early Paleozoic subduction. *Acta Geologica Sinica* 77, 318–327 (in Chinese with English abstract).
- [44] Zhang C., Liu S.W., Han B.F., He G.Q. Huang B.L., 2007a. SHRIMP U-Pb dating of Dashigou biotite-K-felspar granites in Shangdu, Inner Mongolia, and its significance. *Acta Petrologica Sinica* 23(3), 591–596 (in Chinese with English abstract).
- [45] Zhang S.H., Zhao Y., Song B., Yang Z.Y., Hu J.M., Wu H., 2007b. Carboniferous granitic plutons from the northern margin of the North China block: Implications for a Late Paleozoic active continental margin. *Journal of the Geological Society London* 164, 451–463.
- [46] Boynton W.V., 1984. Geochemistry of the rare earth elements: meteorite studies. In: Henderson P. (Ed.), *Rare Earth Element Geochemistry*. Elsevier, 63–114.
- [47] Sun S.S., McDonough W.F., 1989. Chemical and isotope systematics of oceanic basalts: implications for mantle composition and processes. Geological Society, London, *Special Publications* 42, 313–345.
- [48] Martin H., 1986. Effect of steeper Archean geothermal gradient on geochemistry of subduction-zone magmas. *Geology* 14(9), 753–756.
- [49] Drummond M.S., Defant M.J., 1990. A model for trondhjemite-tonalite-dacite genesis and crustal growth via slab melting: Archean to modern comparisons. *Journal of Geophysical Research: Solid Earth* (1978–2012), 95(B13), 21503–21521.
- [50] Stern C.R., Kilian R., 1996. Role of the subducted slab, mantle wedge and continental crust in the generation of adakites from the Andean Austral Volcanic Zone. *Contributions to Mineralogy and Petrology* 123(3), 263–281.
- [51] Kay S.M., Ramos V.A., Marquez M., 1993. Evidence in Cerro Pampa volcanic rocks of slab melting prior to ridge trench collision in southern South America. *Journal of Geology* 101, 703–714.
- [52] Pearce J.A., Harris N.B.W., Tindle A.G., 1984. Trace-element discrimination diagrams for the tectonic interpretation of granitic rocks. *Journal of Petrology* 25, 956–983.
- [53] Atherton M.P., Petford N., 1993. Generation of sodium-rich magmas from newly underplated basaltic crust. *Nature* 362, 144–146.
- [54] Castillo P.R., Janney P.E., Solidum R.U., 1999. Petrology and geochemistry of Camiguin Island, southern Philippines: insights to the source of adakites and other lavas in a complex arc setting. *Contributions to Mineralogy and Petrology* 134, 33–51.
- [55] Castillo P.R., 2006. An overview of adakite petrogenesis. *Chinese Science Bulletin* 51, 257–268.

- [56] Gao S., Rudnick R.L., Yuan H.L., Liu X.M., Liu Y.S., Xu W.L., Ling W.L., Ayers J., Wang X.C., Wang Q.H., 2004. Recycling lower continental crust in the North China craton. *Nature* 432, 892–897.
- [57] Peacock S.M., Rushmer T., Thompson A.B., 1994. Partial melting of subducting oceanic crust. *Earth and Planetary Science Letters* 121, 227–244.
- [58] Drummond M.S., Defant M.J., Kepezhinskas P.K., 1996. Petrogenesis of slab derived trondhjemite-tonalite-dacite/adakite magmas. *Geological Society of America Special Papers* 315, 205–215.
- [59] Defant M.J., Xu J.F., Kepezhinskas P., Wang Q., Zhang Q., Xiao L., 2002. Adakites: some variations on a theme. *Acta Petrologica Sinica* 18, 129–142.
- [60] Kay S.M., Mpodozis C., 2002. Magmatism as a probe to the Neogene shallowing of the Nazca plate beneath the modern Chilean flat-slab. *Journal of South American Earth Sciences* 15, 39–57.
- [61] Rapp R.P., Watson E.B., Miller C.F., 1991. Partial melting of amphibolite/eclogite and the origin of Archean trondhjemites and tonalites. *Precambrian Research* 51, 1–25.
- [62] Rapp R.P., Watson E.B., 1995. Dehydration melting of metabasalt at 8–32 kbar: implications for continental growth and crust-mantle recycling. *Journal of Petrology* 36, 891–931.
- [63] Harris N.B.W., Pearce J.A., Tindle A.G., 1986. Geochemical characteristics of collision zone magmatism. In: Coward M.P., Ries A.C. (Eds.), *Collision Tectonics: Geological Society Special Publications* 19, 67–81.
- [64] Pearce J.A., 1996. Sources and settings of granitic rocks. *Episodes* 19, 120–125.
- [65] Isozaki Y., 1996. Anatomy and genesis of a subduction-related orogen: A new view of geotectonic subdivision and evolution of the Japanese Islands. *Island Arc* 5, 289–320.
- [66] Zhang Y., Tang K., 1989. Pre-Jurassic tectonic evolution of intercontinental region and the suture zone between the North China and Siberian platforms. *Journal of South East Asian Earth Sciences* 3, 47–55.
- [67] Yan Z.Y., Tang K.D., Bai J.W., Mo Y.C., 1989. High pressure metamorphic rocks and their tectonic environment in northeastern China. *Journal of Southeast Asian Earth Sciences* 3, 303–313.
- [68] Shi Y.R., Liu D.Y., Jian P., Zhang Q., Zhang F.Q., Miao L.C., Shi G.H., Zhang L.Q., Tao H., 2005b. Zircon SHRIMP dating of K-rich granites in Sonid Zuoqi, Central Inner Mongolia. *Geological Bulletin of China* 25, 424–428 (in Chinese with English abstract).
- [69] Shi Y.R., Liu D.Y., Miao L.C., Zhang F.Q., Jian P., Zhang W., Hou K.J., Xu J.Y., 2010. Devonian A-type granitic magmatism on the northern margin of the North China Craton: SHRIMP U-Pb zircon dating and Hf-isotopes of the Hongshan granite at Chifeng, Inner Mongolia, China. *Gondwana Research* 17(4), 632–641.

- [70] Zhang S.H., Zhao Y., Song B., Hu J.M., Liu S.W., Yang Y.H., 2009. Contrasting Late Carboniferous and Late Permian-Middle Triassic intrusive suites from the northern margin of the North China craton: Geochronology, petrogenesis, and tectonic implications. *Geological Society of America Bulletin* 121(1–2), 181–200.
- [71] Ni Z.Y., Zhai M.G., Wang R.M., Tong Y., 2006. Late Paleozoic retrograded eclogites from within the northern margin of the North China Craton: evidence for subduction of the Paleo-Asian ocean. *Gondwana Research* 9, 209–224.
- [72] Stern R.J., Bloomer S.H., 1992. Subduction zone infancy: examples from the Eocene Izu-Bonin-Mariana and Jurassic California arcs, *Geological Society of America Bulletin* 104, 1621–1636.